Control of the low-load region in partially premixed combustion

Gabriel Ingesson[1], Lianhao Yin[2], Rolf Johansson[1] and Per Tunestål[2]

[1]Department of Automatic Control, Lund University, Lund, Sweden
[2]Department of Energy Sciences, Lund University, Lund, Sweden

E-mail: Gabriel.Ingesson@control.lth.se

Abstract. Partially premixed combustion (PPC) is a low temperature, direct-injection combustion concept that has shown to give promising emission levels and efficiencies over a wide operating range. In this concept, high EGR ratios, high octane-number fuels and early injection timings are used to slow down the auto-ignition reactions and to enhance the fuel and are mixing before the start of combustion. A drawback with this concept is the combustion stability in the low-load region where a high octane-number fuel might cause misfire and low combustion efficiency. This paper investigates the problem of low-load PPC controller design for increased engine efficiency. First, low-load PPC data, obtained from a multi-cylinder heavy-duty engine is presented. The data shows that combustion efficiency could be increased by using a pilot injection and that there is a non-linearity in the relation between injection and combustion timing. Furthermore, intake conditions should be set in order to avoid operating points with unfavourable global equivalence ratio and in-cylinder temperature combinations. Model predictive control simulations were used together with a calibrated engine model to find a gas-system controller that fulfilled this task. The findings are then summarized in a suggested engine controller design. Finally, an experimental performance evaluation of the suggested controller is presented.

1. Introduction

Partially premixed combustion (PPC) is a low temperature combustion concept with the direct controllability of the combustion timing through fuel injection. Low temperature combustion is an often used name for combustion concepts where the ignition delay is prolonged in direct-injection engines in order to enhance fuel-air premixing. An increased ignition delay gives the fuel more time to penetrate the gas mixture before the combustion starts. This yields locally leaner mixtures during combustion which both reduces the formation of particulate matter and NO_x due to lower combustion temperatures [1].

In PPC, a combination of early injection timings, high exhaust-gas recirculation (EGR) ratios and the usage of gasoline-like fuels is applied to achieve a sufficiently long ignition delay while maintaining low fuel consumption [2].

One of the problems with gasoline PPC is the combustion stability and efficiency at low load. The advantage with higher octane-number fuels have mainly been observed at high-load operating conditions. At low load, the high octane-number fuels are difficult to ignite and the emissions levels of HC and CO are high.

It was showed in [2] that the low-load limit for PPC, defined as the load for which the

combustion was not stable at atmospheric intake conditions, increased from 3 to 15 bar as the fuel RON increases from 70 to 100, in a single-cylinder, heavy-duty engine.

Homogeneous reactor simulations at constant temperature and pressure for various equivalence ratios and temperatures show that high HC emission levels is a result of lean mixtures at too low temperature, [3]. Results in [4] and [5] showed that a sufficiently stratified charge can be essential for efficient combustion. A remedy to the low-load problem of PPC could thus be to increase in-cylinder temperature and stratification levels.

Previous light-duty engine studies, presented in [6] and [7] aimed to improve the PPC low-load combustion stability and efficiency using variable-valve actuation while running on a 87 RON fuel. The results showed that strategies using negative valve overlap, rebreathing and split main-fuel injection were able to increase the low-load performance.

In [8], the low-load limit of a single cylinder light duty engine at 1500 rpm engine speed was extended down to 2 bar gross indicated mean effective pressure, p_{IMEPg}, using boosted inlet air. The absolute inlet pressure at 2 bar p_{IMEPg} was approximately 2 bar for the fuels with the highest RON (88.6 and 87.1) with 53 % EGR level. HC and CO emissions were higher with the higher RON value gasoline fuels.

This paper studies low-load gasoline PPC operation from a controller design perspective, where fuel-injection timing, pilot-injection amount, EGR and thermal-management actuation are used to improve combustion efficiency in a 13 liter, heavy-duty engine. Experimental data from the load range 1-5 bar net-indicated mean-effective pressure, p_{IMEPn}, with different fuel-injection and gas-exchange system configurations is presented in the first section. A suggested controller design that aims to maximize the net indicated efficiency is then presented in the following sections. The suggested engine controller consists of combustion-timing PI controllers that aim to phase the combustion timing shortly after top-dead-center (TDC), while operating in a region where the combustion timing is controllable. A pilot injection is also introduced close to the main-fuel injection in order to improve combustion efficiency. A static gas-system feedback controller was found from offline model predictive control simulations using a calibrated gas-system model. The found gas-system controller varies the gas-exchange valve positions in order to keep the combustion away from conditions where the global equivalence-ratio, ϕ, and in-cylinder temperature, T, are less favourable. The simulation and model-calibration procedures are also presented in the paper.

Finally, experimental controller-evaluation tests during load-step changes are presented in the last section.

2. Experimental Setup

2.1. Engine Specifications

The experimental engine was a Scania D13 heavy-duty diesel engine with engine specifications displayed in table 2.1. The engine speed was controlled with a 355 kW AC motor that worked both as an engine motor and brake. The engine was boosted with a fixed-geometry turbocharger. The intake temperature was controlled by a cooled air-path valve prior to the intake-manifold and a EGR valve is used to control the EGR flow, see Fig. 1.

2.2. Engine control and measurement system

The entire engine control system was programmed with LabVIEW which is a graphical programming environment developed by National Instruments. The real-time system consisted of a NI PXIe-8135 embedded controller (2.3 GHz quad-core processor), NI PXI-7854/7854 R (Multifunction reconfigurable I/O (RIO) with Virtex 5-LX110/LX30 FPGA). The FPGA was considered as a configurable hardware that worked as a flexible AO / DIO and was also used for AD acquisition.

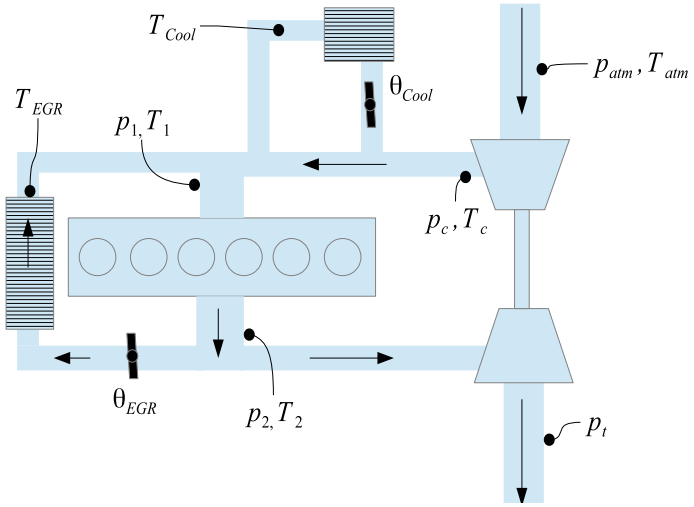

Figure 1. The gas-exchange system. The engine was boosted by a fixed-geometry turbocharger. The gas-system actuators consisted of the cooled air-path valve position, θ_{Cool}, located prior to the intake manifold and the cooled-EGR valve position, θ_{EGR}.

The in-cylinder pressure was measured with water-cooled Kistler 7061B pressure sensors and was sampled with the Leine-Linde crank angle encoder pulse every 0.2 crank angle degree. Inlet manifold and exhaust pressures were measured with Keller PAA-23S absolute pressure sensors. Inlet manifold and exhaust temperatures were measured with K-type thermocouples.

The fuel injection system was a production Xtra high Pressure Injection (XPI) common-rail injection system for the Scania D13 engines. The common-rail pressure, injection timings, durations and valve positions were controlled from the real-time system using Drivven drivers. The fuel used in the experiments was a mixture of 80 volume % gasoline and 20 volume % N-heptane.

The heat-release analysis and controller computations were run in MathScript RT Module nodes inside a timed-loop block on the real-time target. The timed loop was triggered by the FPGA once the in-cylinder pressures were sampled. All computations were done using floating point arithmetic.

Table 1. Engine Specifications

Total Displaced volume	12.74 dm^3
Stroke	160 mm
Bore	130 mm
Connecting Rod	255 mm
Compression ratio	18:1
Number of Valves	4

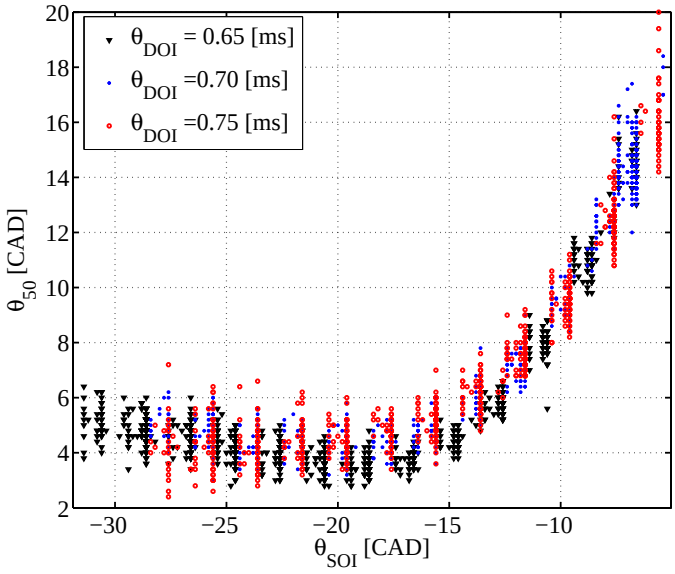

Figure 2. Combustion timing, θ_{50}, as a function of fuel-injection timing, θ_{SOI}, for three different fuel-injection durations, θ_{DOI}. For injections closer to TDC the gain between θ_{SOI} and θ_{50} is positive. As θ_{SOI} is advanced, the gain decreases and for very advanced θ_{SOI}, it becomes slightly negative. This negative gain is more significant for the shorter injection durations.

3. Low-Load Experiments

This section presents experimental data that describes the combustion sensitivity to injection-timing, pilot-injection amount and intake conditions. The results present the difficulties with PPC low-load control and provides a foundation for the controller design.

3.1. Injection Timing

In order to achieve high thermodynamic efficiency and acceptable combustion stability, the combustion timing has to be phased shortly after TDC, the combustion timing is here defined as the crank-angle degree of 50 % burnt, θ_{50}, here computed from the measured in-cylinder pressure p using the equation for the gross apparent rate of heat release $dQ_g/d\theta$, [9],

$$\frac{dQ_g}{d\theta} = \frac{\gamma}{\gamma - 1} p \frac{dV}{d\theta} + \frac{1}{\gamma - 1} V \frac{dp}{d\theta} \tag{1}$$

where V is the in-cylinder volume, θ is the crank angle and γ is the ratio of specific heats.

Experimentally obtained θ_{50} is presented in Fig. 2 as a function of injection timing, θ_{SOI}, for three different fuel-injection durations, θ_{DOI}, with a common-rail pressure at 800 bar. For θ_{SOI} closer to TDC, the gain from θ_{SOI} to θ_{50} is positive. As θ_{SOI} is advanced, the gain decreases and for very advanced θ_{SOI}, the gain becomes negative. Similar trends for different fuels were presented in [4]. The data gives a lower bound for which θ_{SOI} can be used to control θ_{50} effectively. From these results it was decided to control θ_{50} with θ_{SOI} using a PI controller with manually tuned gains, where θ_{SOI} was kept above -20 CAD after TDC in order to stay in the non-negative gain region, θ_{50} was then controlled to stay at 5 CAD after TDC.

3.2. Pilot Injection

It has previously been shown that a pilot injection can be used to improve combustion stability [10], [11] and to decrease the ignition delay of the main injection, [12] which increases the

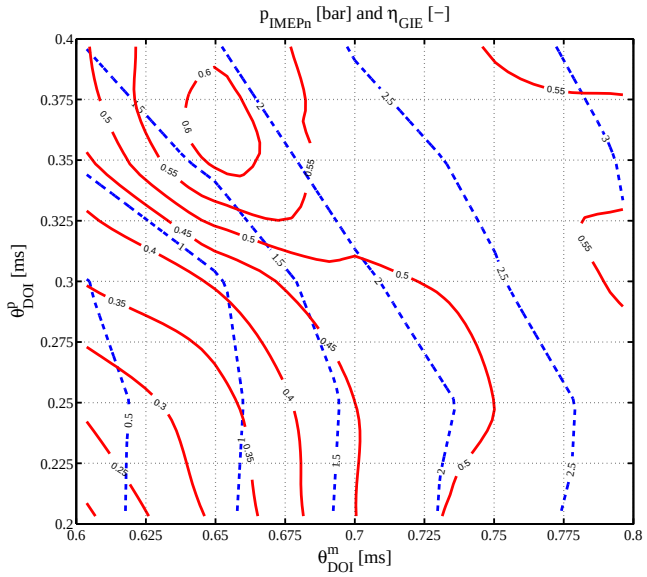

Figure 3. Level curves of p_{IMEPg} (blue, dashed) and η_{GIE} (red, solid) as a function of θ^m_{DOI} and θ^p_{DOI}. By following p_{IMEPn} level curve, η_{GIE} can be increased by having a higher θ^p_{DOI} relative to θ^m_{DOI}. This trend is stronger for the low-load level curves.

stratification levels during combustion. Experiments with different pilot and main fuel injection durations θ^p_{DOI}, θ^m_{DOI} were conducted in order to investigate the θ^p_{DOI} effect on the gross indicated efficiency, η_{GIE}, which is the product of the thermodynamic efficiency η_{th} and the combustion efficiency η_{c}. Here η_{GIE} was computed according to

$$\eta_{\mathrm{GIE}} = \eta_{\mathrm{th}}\eta_{\mathrm{c}} = \frac{p_{\mathrm{IMEPg}} V_d}{Q_{\mathrm{LHV}} m_f}, \tag{2}$$

where V_d is the displacement volume, Q_{LHV} is the lower heating value of the fuel and m_f is the injected fuel amount, computed from steady-state fuel-flow measurements. During the experiments θ_{50} was kept as close to TDC as possible while the pilot injection was positioned 20 CAD prior to the main injection. Level curves of p_{IMEPn} (blue, dashed) and η_{GIE} (red, solid) as a function of θ^m_{DOI} and θ^p_{DOI} are presented in Fig. 3. When traveling along a lower value, p_{IMEPg} level curve, η_{GIE} can be increased by having a higher θ^p_{DOI} in relation to θ^m_{DOI}. As p_{IMEPg} is increased, this effect becomes less significant.

From these results it was concluded that the controller should keep a constant pilot duration, $\theta^p_{\mathrm{DOI}} = 0.4$, positioned 20 CAD before the main injection in order to increase η_{GIE}.

3.3. Intake Conditions

In order to investigate the effect of intake conditions, the gas-system valve positions, θ_{EGR} and θ_{Cool}, were varied in every different combination from closed to open for the different θ^m_{DOI},

$$\theta^m_{\mathrm{DOI}} = \begin{pmatrix} 0.65 & 0.7 & 0.75 & 0.85 & 1.05 \end{pmatrix}. \tag{3}$$

The combustion phasing, θ_{50}, was kept in the region 5-10 CAD and no pilot injection was used. A part of the obtained data is presented as the black lines in Fig. 6. In Fig. 4, η_{GIE} is presented as a function of equivalence ratio ϕ and temperature at θ_{SOI}, $T_{\theta_{\mathrm{SOI}}}$, computed using the adiabatic

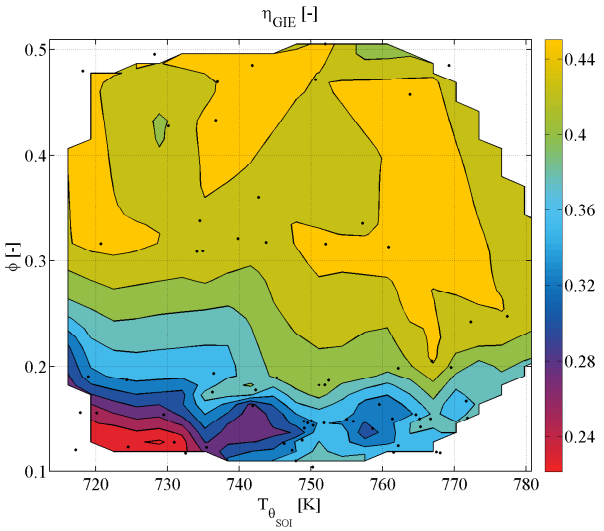

Figure 4. Experimental η_{GIE} as a function of equivalence ratio ϕ and temperature at θ_{SOI}. For low ϕ, the efficiency can be increased by increasing the temperature. This data was used to model η_{NIE} in the model predictive control simulations presented in a following section.

compression relation during the compression stroke

$$T_{\theta_{\mathrm{SOI}}} = T_2(\theta_{\mathrm{IVC}}) \left(\frac{V(\theta_{\mathrm{IVC}})}{V(\theta_{\mathrm{SOI}})} \right)^{\gamma - 1} \tag{4}$$

where $T_2(\theta_{\mathrm{IVC}})$ is the measured intake manifold temperature at inlet-valve closing (IVC). For low ϕ, η_{th} is more sensitive to $T_{\theta_{\mathrm{SOI}}}$ and could be increased significantly by heating the in-cylinder gas mixture.

Varying θ_{EGR} and θ_{Cool} also affects the pumping losses, p_{PMEP}, which is the indicated mean-effective pressure during the gas-exchange strokes. The measured relation between p_{PMEP} and the intake and exhaust manifold pressures, p_{in}, p_{ex}, is presented in Fig. 5. The net-indicated efficiency η_{NIE} is computed according to

$$\eta_{\mathrm{GIE}} = \eta_{\mathrm{th}} \eta_{\mathrm{c}} = \frac{(p_{\mathrm{IMEPg}} + p_{\mathrm{PMEP}}) V_d}{Q_{\mathrm{LHV}} m_f}. \tag{5}$$

The data in Figs. 4 and 5 was used for simulation and offline efficiency-optimization, this will be covered in the following sections.

4. Gas-System Modeling

Model-based optimal control was used in simulation to find efficient actuation of the gas-system valve positions, θ_{EGR} and θ_{Cool}. However, in order to do this, a mathematical description of the gas-exchange system (illustrated in Fig. 1) was needed. It was decided to use a system of ordinary differential equations to model the pressures and temperatures in the different gas-system volumes and the flow between them, an approach that has previously been found to be successful for controller-design purposes, for instance in [13] and [14].

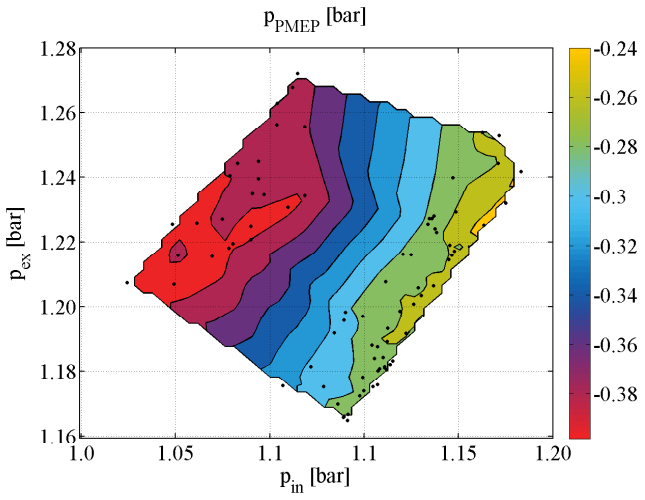

Figure 5. Experimental p_{PMEP} as a function of intake and exhaust-manifold pressures, p_{in}, p_{ex}. This data was used to model η_{NIE} in the model predictive control simulations presented in a following section.

4.1. System Equations

The pressure, p_i, and temperature, T_i, of the gas-system volumes (see Fig. 1) were modelled using the adiabatic volume equations, [15].

$$\frac{dp_i}{dt} = \frac{RT_i}{V_i}(\dot{W}_{\text{in}} - \dot{W}_{\text{out}}) + \frac{p_i}{T_i}\frac{dT_i}{dt}, \tag{6}$$

$$\frac{dT_i}{dt} = \frac{RT_i}{V_i p_i c_v}(c_v(\dot{W}_{\text{in}}T_{\text{in}} - \dot{W}_{\text{in}}T_i) + R(\dot{W}_{\text{in}}T_{\text{in}} - \dot{W}_{\text{out}}T_i)).$$

Where $\dot{W}_{\text{in}}$ and $\dot{W}_{\text{out}}$ is the total in- and outgoing mass flow respectively. The mass flow from volume i to volume j, $\dot{W}_{i\to j}$ was modeled as a compressible flow through a restriction, [15],

$$\dot{W}_{i\to j} = \frac{A_{i\to j}p_i}{\sqrt{RT_i}}\Psi(\Pi_{i,j}), \tag{7}$$

where $A_{i\to j}$ is the flow area R the ideal gas constant, Ψ and Π are given by

$$\Psi(\frac{p_j}{p_i}) = \sqrt{\frac{2\gamma}{\gamma-1}\left((\Pi_{i,j})^{2/\gamma} - (\Pi_{i,j})^{1+1/\gamma}\right)} \tag{8}$$

and

$$\Pi_{i,j} = \begin{cases} \left(\frac{2}{\gamma+1}\right)^{\frac{\gamma}{\gamma-1}} & \text{if } \frac{p_j}{p_i} < \left(\frac{2}{\gamma+1}\right)^{\frac{\gamma}{\gamma-1}}, \\ \frac{p_j}{p_i} & \text{if } \left(\frac{2}{\gamma+1}\right)^{\frac{\gamma}{\gamma-1}} \le \frac{p_j}{p_i} \le 1, \\ 1 & \text{if } 1 < \frac{p_j}{p_i}. \end{cases} \tag{9}$$

The mass flow from the intake manifold to the cylinders were modeled using a volumetric efficiency η_v

$$\dot{W}_{\text{cyl}} = \eta_v \frac{N_{\text{speed}}p_1 V_d}{120RT_1} \tag{10}$$

where

$$\eta_v = \frac{r_c - (\frac{p_1}{p_2})^{1/\gamma}}{r_c - 1} \tag{11}$$

and N_{speed} is the engine speed in rpm. The compressor power was modeled assuming first assuming the relation for the turbine-power, P_t,

$$P_t = \eta_{\text{th}}^t c_v T_2 (1 - \frac{p_t}{p_2})^{1-1/\gamma} \dot{W}_t, \tag{12}$$

where η_{th}^t is the turbine thermodynamic efficiency, and $\dot{W}_t$ is the flow over the turbine. The compressor power, P_c was then computed with a mechanical efficiency η_{c} and the static relation

$$P_c = \eta_{\text{c}} P_t. \tag{13}$$

The flow over the compressor, $\dot{W}_c$, was then given by the equation

$$\dot{W}_c = \frac{\eta_c P_c}{T_{\text{atm}} c_v (\frac{p_c}{p_{\text{atm}}} - 1)^{1-1/\gamma}}. \tag{14}$$

a similar model was presented in [14]. The relations between valve positions θ_{Cool}, θ_{EGR} and the flow areas A_{EGR}, A_{Cool} was modeled using the following empirical equations

$$A_{\text{EGR}} = A_1(1 - e^{-k_1 \theta_{\text{EGR}}}), \tag{15}$$

$$A_{\text{Cool}} = A_2(1 - e^{-k_2 \theta_{\text{Cool}}}),$$

where A_1, A_2 and k_1, k_2 are calibration parameters.

Engine-out temperature T_{EO} and the cooler flow temperatures T_{EGR}, T_{Cool} was modelled using second-order polynomials c_i in two variables

$$T_{\text{EO}}(m_f, T_1) = c_1(m_f, T_1), \tag{16}$$

$$T_{\text{EGR}}(T_2, \dot{W}_{\text{EGR}}) = c_2(T_2, \dot{W}_{\text{EGR}}),$$

$$T_{\text{Cool}}(T_2, \dot{W}_{\text{EGR}}) = c_3(T_c, \dot{W}_{\text{Cool}}).$$

4.2. Model Calibration

In order to calibrate the model w.r.t. the unknown parameters, the polynomial coefficients in c_{1-3}, k_1 and k_2 were first calibrated w.r.t. flow and temperature data. The unknown variables,

$$\vartheta = \begin{pmatrix} A_1 & A_2 & A_t & \eta^t \eta^c \end{pmatrix}^T \tag{17}$$

ϑ, were then computed by minimizing the model-output error cost function $V(\vartheta)$,

$$V(\vartheta) = \|p_1^m - p_1\|_2^2 + \|p_2^m - p_2\|_2^2 + \|p_c^m - p_c\|_2^2 \tag{18}$$

$$+ \beta(\|T_1^m - T_1\|_2^2 + \|T_2^m - T_2\|_2^2),$$

where p_i^m, T_i^m are measured pressure and temperature data and p_i, T_i are simulated model output. The minimization was done subject to $\eta^t \eta^c \leq 1$ and measured boundary conditions p_{atm}, T_{atm}, p_{t}. In V, $\|\cdot\|$ is the Euclidian norm and the parameter β determines the relative importance between fitting temperature and pressure. Model output and measured data are shown in Fig. 6 for a local minimizer ϑ^* of (18), found using Matlab's nonlinear optimization toolbox.

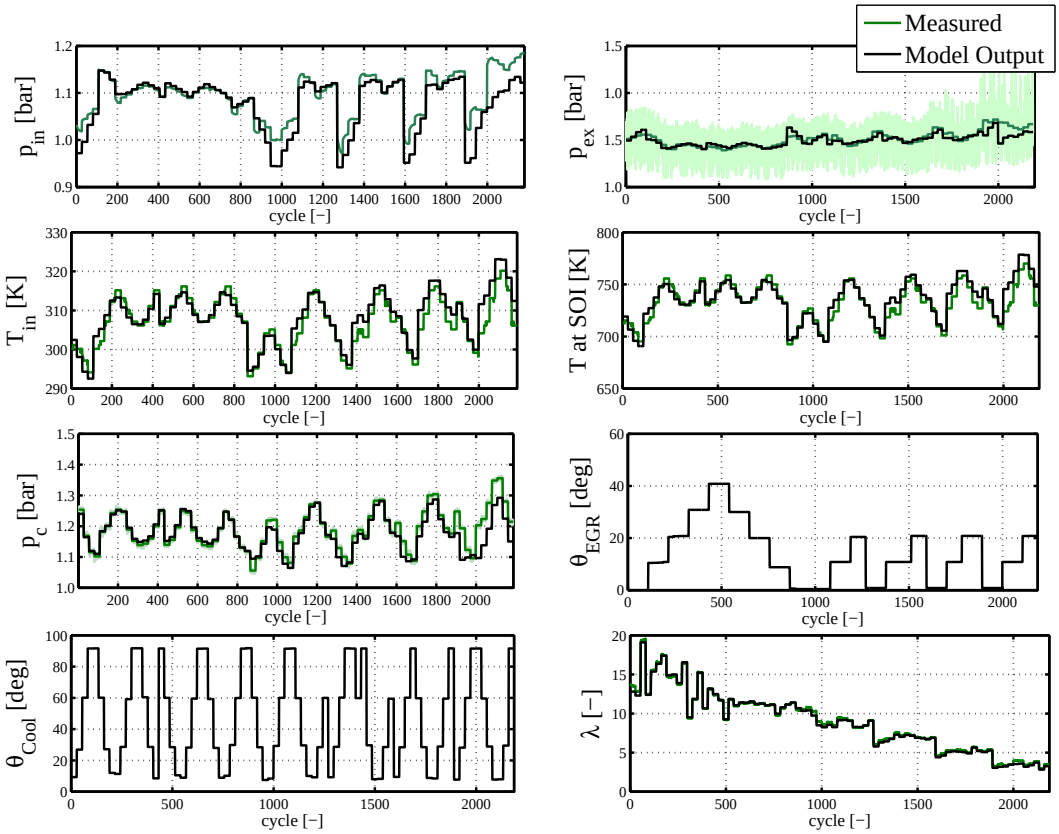

Figure 6. Model output (black) and measured data (green) for a local minimizer ϑ^*.

5. Gas-System Controller Design

The obtained calibrated gas-system model was then used to find optimal control action for θ_{Cool} and θ_{EGR} during p_{IMEPn} set-point changes. For this purpose, the principle of model predictive control (MPC) was used.

MPC is a finite-horizon optimal-control principle where the input sequence $\mathcal{U} = [u(k), \ldots, u(k + H_p - 1)]^T$ from sample k to H_p is computed iteratively at every new sample k by solving an optimization problem, the first input $u^*(k)$ of the optimal sequence $\mathcal{U}^*$ is actuated to the system each sample, [16]. MPC, also known as receding-horizon control and dynamic programming, has previously been applied to a wide range of problems including chemical-process control [16], supply-chain management [17], finance [18] and internal-combustion engines [19], [20].

The MPC optimization problem to be solved every sample k, in this case cycle k was formulated accordingly

$$\underset{\theta_{\text{Cool}},\theta_{\text{EGR}}}{\text{minimize}}\ J(\theta_{\text{Cool}},\theta_{\text{EGR}},\phi,T_{\theta_{\text{SOI}}},p_1,p_2,m_f) \tag{19}$$

$$=\sum_{k=1}^{H_p}\omega_1|m_f(k)|+\omega_2||90-\theta_{\text{Cool}}(k)||_2^2+\omega_3||\theta_{\text{EGR}}(k)||_2^2$$

$$\text{subject to}\ \ l_b\leq\begin{pmatrix}\theta_{\text{EGR}}\\ \theta_{\text{Cool}}\\ \Delta\theta_{\text{EGR}}\\ \Delta\theta_{\text{Cool}}\end{pmatrix}\leq u_b,$$

$$\dot{x}=f(x,\theta_{\text{Cool}},\theta_{\text{EGR}}),$$

$$x=\begin{pmatrix}p_1 & p_2 & p_c & T_1 & T_2\end{pmatrix}^T,$$

$$\eta_{\text{GIE}}=g_1(\phi,T_{\theta_{\text{SOI}}}),$$

$$p_{\text{PMEP}}=g_2(p_1,p_2),$$

where g_1 and g_2 are obtained by interpolating the data in Figs. 4 and 5. The two second terms in the cost function were introduced so that the controller would only heat the intake air at low-load operating points. The cost-function weights ω_{1-3} then determine the valve control action for a lowered fuel consumption.

MPC simulation experiments were studied where p_{IMEPn} was set to follow a predetermined set-point trajectory, controlled using a PI controller, the effects of variations in θ_{50} were not considered as it was assumed to be held constant. The MPC optimization problem (19) was solved each cycle using Matlab's nonlinear optimization toolbox and the ode23s solver to compute the gas-system model output.

Simulation results for three different controllers with $\omega_1 = 0$, 1, 5, $\omega_2 = \omega_3 = 10$ and $H_p = 10$ are presented in Fig. 7. As the cost for fuel consumption is increased, θ_{Cool} closes and θ_{EGR} opens in order to avoid the low-efficiency region in the $\phi - T$ map, it is seen that this lowers the needed fuel amount in low-load operation. For the third controller in Fig. 7, it was found that θ_{Cool} and θ_{EGR} almost fulfilled a static feedback law in ϕ, see Fig 8 where simulation data and an approximate static feedback law K,

$$\begin{pmatrix}\theta_{\text{Cool}}\\ \theta_{\text{EGR}}\end{pmatrix}=K(\phi), \tag{20}$$

is presented. It was decided to use the full range of θ_{Cool} which gives a deviation for high ϕ.

6. Engine-Controller Design

The previously presented gave the following suggested engine controller:

- Combustion timing, θ_{50}, is controlled by θ_{SOI} using PI controllers where θ_{SOI} is limited to the positive-gain region in Fig.2. This is done in order to ensure θ_{50} controllability.
- A pilot injection with a duration of 0.4 ms is introduced in order to increase combustion efficiency, motivated by the result presented in Fig. 3.
- The gas-exchange valves are set according to the feedback law $K(\phi)$, derived from data-based engine simulation and optimal control. In this work, ϕ was computed using the previously presented cylinder flow model and pre-calibrated injected fuel mass flow from the injection durations.

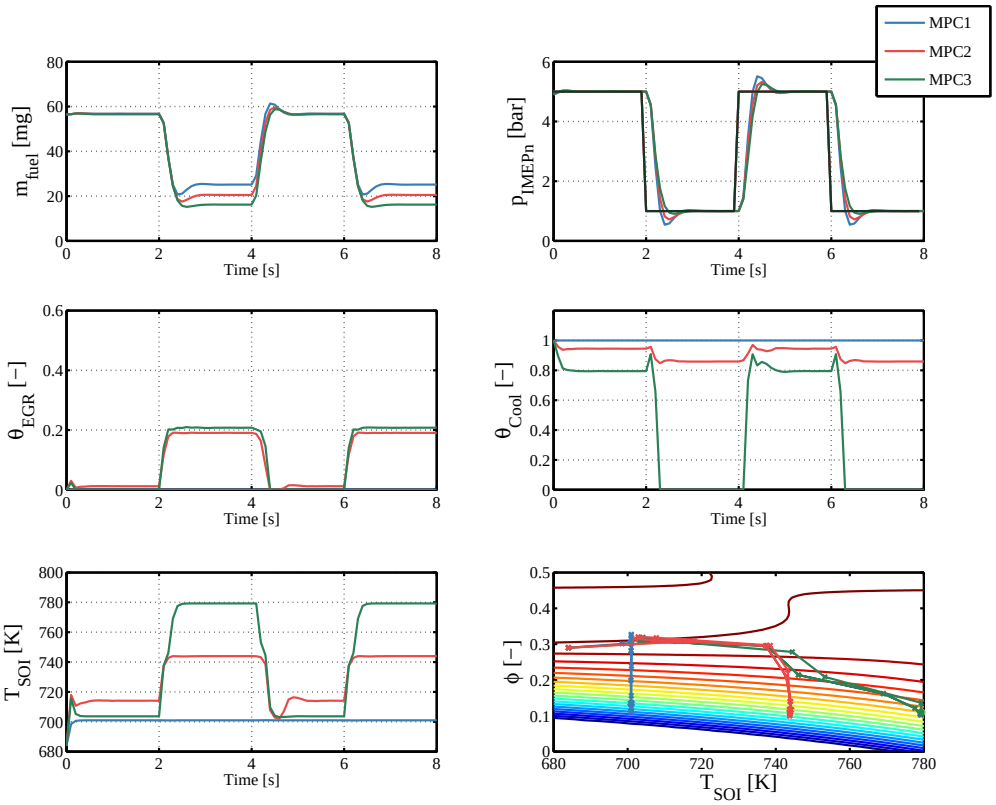

Figure 7. Simulated MPC output for different choices of fuel consumption penalty, for higher penalty, the controller avoids the low efficiency region in the $\phi - T$ map, this can be seen in the lower right subfigure where level curves represents η_{GIE} obtained from the data in Fig. 4.

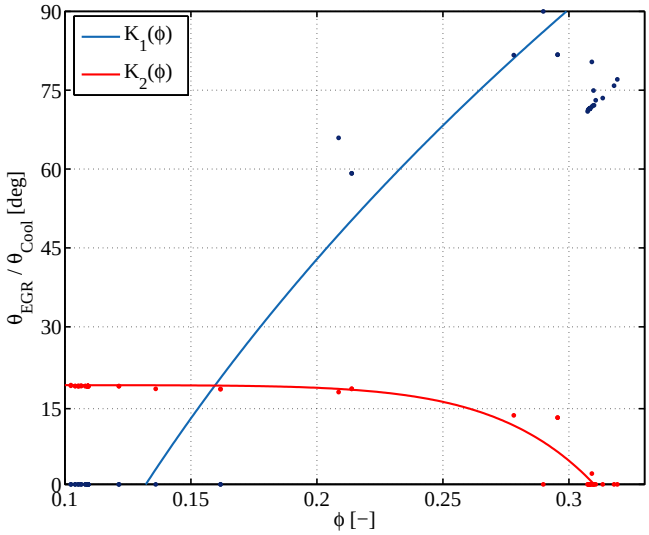

Figure 8. MPC-simulation θ_{EGR} and θ_{Cool} and an approximate static feedback law K, it was decided to use the full range of θ_{Cool} which gives a deviation for high ϕ.

7. Controller Evaluation

Finally, the suggested controller was evaluated experimentally during a test cycle where p_{IMEPn} was set to follow set-point changes at constant engine speed. In order to compare performance, four different controller cases were evaluated.

(i) Cylinder-individual θ_{50} PI controllers.

(ii) Cylinder-individual θ_{50} PI controllers, where θ_{SOI} was limited to the positive-gain region.

(iii) Case (ii) with a pilot-fuel injection.

(iv) Case (iii) with the the gas-system feedback law $K(\phi)$.

For all cases, p_{IMEPg} was controlled by keeping the rail-pressure constant and varying the main-injection duration, this was accomplished using a separate controller.

Experimental test-cycle results from one of the cylinders for the four different cases are presented in Fig. 9. In case (i), the injection timing is not limited to the positive-gain region which leads to very early injection timings, and as a result, an retarded θ_{50}. When introducing a pilot injection, the ignition delay is decreased, see the θ_{SOI}, θ_{50} subfigures. This makes θ_{SOI} more easily controlled and more advanced combustion timings can be achieved. Finally, in case (iv), the ignition delay is further decreased as the intake temperature is increased when θ_{EGR} increases and θ_{Cool} decreases for the low-load operating points. The accumulated injected fuel mass, computed from fuel-injection durations is presented in Fig. 10, the fuel-consumption rates differ more clearly at low-load operating point, both introducing a pilot injection and heating the intake temperature lower the fuel consumption.

8. Conclusions

This paper presents an engine-control strategy for improved PPC low-load performance. The combustion timing θ_{50} is only controllable w.r.t. θ_{SOI} in a specific region, see Fig.2, therefore it is important to avoid this region so that a feedback controller does not go for extremely early injection timings when controllability is lost, see Fig. 9. Adding a pilot injection showed to increase the combustion efficiency at low load both in steady state and transient operation, see Figs. 3 and 10. This is believed to be caused by the fact that the pilot injection decreases the ignition delay of the main injection which leads to more stratified combustion mixtures which is more favorable at low global ϕ. The combustion efficiency could also be increased by heating the inducted air charge, see Fig. 4 and this was done by operating θ_{EGR} and θ_{Cool} according to a feedback-law, $K(\phi)$, obtained from offline model predictive control simulations.

Acknowledgments

The authors would like to acknowledge the Competence Center for Combustion Processes, KCFP, and the Swedish Energy Agency for the financial support (project number 22485-3), Scania for supplying the experimental engine and the KFCP PPC Control reference group for consistent feedback on the work. The authors Ingesson and Johansson are members of the LCCC Linnaeus Center and the eLLIIT Excellence Center at Lund University.

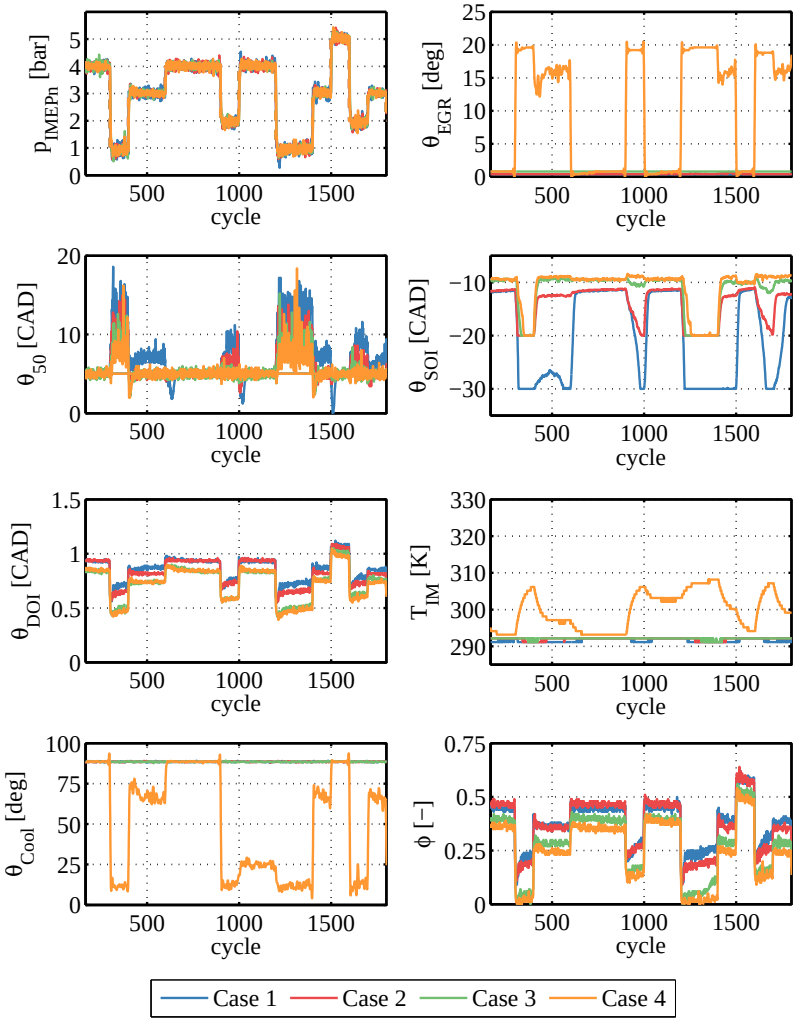

Figure 9. Experimental results for the three different cases. In case 1, the injection timing is not limited to the positive-gain region which leads to very early injection timings, and as a result, a retarder combustion phasing. When introducing a pilot injection, the ignition delay is decreased which can be seen in the θ_{SOI}, θ_{50} subfigures. This makes θ_{SOI} more easily controlled. Finally, in case 4, the ignition delay is increased further as the intake temperature is increased as θ_{EGR} increases and θ_{Cool} decreases for the low-load operating points.

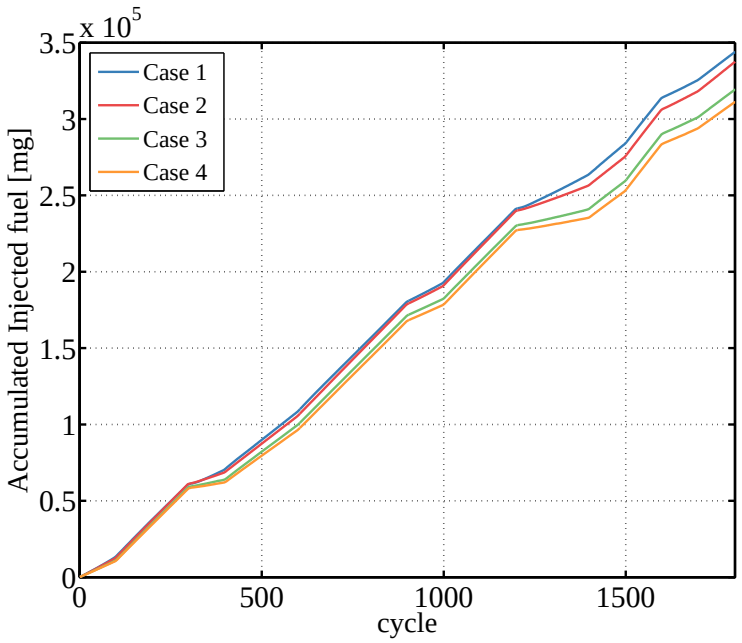

Figure 10. Accumulated injected fuel mass for the four cases in Fig. 9. The slopes of the curves differ more the lowest loads, both introducing a pilot fuel injection and heating the intake lower the fuel consumption. The injected fuel mass was computed from fuel injection timings a relation which was calibrated from previous state state measurements, the reason for not using the mass-flow meter was that it was mounted far from the engine and thus not so reliable in transient operation.

References

[1] Musculus M P 2006 Multiple simultaneous optical diagnostic imaging of early-injection low-temperature combustion in a heavy-duty diesel engine 2006-01-0079 SAE Technical Paper
[2] Manente V, Zander C G, Johansson B, Tunestal P and Cannella W 2010 An advanced internal combustion engine concept for low emissions and high efficiency from idle to max load using gasoline partially premixed combustion 2010-01-2198 SAE Technical Paper
[3] Kim D, Ekoto I, Colban W F and Miles P C 2008 In-cylinder co and uhc imaging in a light-duty diesel engine during ppci low-temperature combustion 2008-01-1602 SAE Technical Paper
[4] Kalghatgi G T, Risberg P and Ångström H E 2006 Advantages of fuels with high resistance to auto-ignition in late-injection, low-temperature, compression ignition combustion 2006-01-3385 SAE Technical Paper
[5] Weall A and Collings N 2009 Gasoline fuelled partially premixed compression ignition in a light duty multi cylinder engine: a study of low load and low speed operation 2009-01-1791 SAE Technical Paper
[6] Borgqvist P, Tunestal P and Johansson B 2012 Gasoline partially premixed combustion in a light duty engine at low load and idle operating conditions 2012-01-0687 SAE Technical Paper
[7] Borgqvist P, Tunestal P and Johansson B 2013 *SAE International Journal of Engines* **6** 366–378
[8] Solaka H, Aronsson U, Tuner M and Johansson B 2012 Investigation of partially premixed combustion characteristics in low load range with regards to fuel octane number in a light-duty diesel engine 2012-01-0684 SAE Technical Paper
[9] Heywood J B 1988 *Internal combustion engine fundamentals* vol 930 (New York: Mcgraw-hill)
[10] MacMillan D, La Rocca A, Shayler P, Morris T, Murphy M and Pegg I 2009 *SAE International Journal of Engines* 2009-01-0612
[11] Osuka I, Nishimura M, Tanaka Y and Miyaki M 1994 Benefits of new fuel injection system technology on cold startability of diesel engines-improvement of cold startability and white smoke reduction by means of multi injection with common rail fuel system ECD-U2 940586 SAE Technical Paper
[12] Manente V, Johansson B and Tunestal P 2009 Partially premixed combustion at high load using gasoline and ethanol, a comparison with diesel 2009-01-0944 SAE Technical Paper
[13] Guzzella L and Onder C 2009 *Introduction to modeling and control of internal combustion engine systems* (Berlin: Springer-Verlag)
[14] Wahlström J and Eriksson L 2011 *Proceedings of the Institution of Mechanical Engineers, Part D: Journal of Automobile Engineering* **225** 960–986
[15] Eriksson L and Nielsen L 2014 *Modeling and control of engines and drivelines* (Chichester, West Sussex, United Kingdom: John Wiley & Sons)
[16] Maciejowski J M 2002 *Predictive control: with constraints* (Essex, England: Pearson Education)
[17] Cho E, Thoney K, Hodgson T and King R 2003 Rolling horizon scheduling of multi-factory supply chains *Simulation Conference, 2003. Proceedings of the 2003 Winter* vol 2 pp 1409–1416 vol.2
[18] Dawid H 2005 *Economic Theory* **25** 575–597
[19] Widd A, Ekholm K, Tunestal P and Johansson R 2009 Experimental evaluation of predictive combustion phasing control in an hcci engine using fast thermal management and VVA *Control Applications, (CCA) Intelligent Control, (ISIC), 2009 IEEE* (Saint Petersburg) pp 334–339
[20] Lewander M, Johansson B, Tunestål P, Keeler N, Milovanovic N and Bergstrand P 2008 Closed loop control of a partially premixed combustion engine using model predictive control strategies *Proceedings of AVEC* vol 8 (Kobe, Japan)